J Mater Sci (2009) 44:3315–3318
DOI 10.1007/s10853-008-3172-2

LETTER

Thickness-induced crystallization of amorphous In_2O_3 films: influence of the film deposition rate

S. Muranaka · N. Hayashi

Received: 27 November 2008 / Accepted: 8 December 2008 / Published online: 14 April 2009

Several authors have studied the crystallization of amorphous In_2O_3 films in order to investigate the application of the films as transparent conductors and to elucidate the kinetics of the crystal growth of the films in general [1–4]. At substrate temperatures of 150–250 °C, the films initially grow in an amorphous form and later crystallize as the film thickness increases [1]. This thickness-induced crystallization of the amorphous films is of interest from the viewpoint of the nucleation and growth of thin films, but little has been reported on the details of the film structure. In this study we applied transmission electron microscopy to investigate the effect of the film thickness on the crystallization of In_2O_3 deposits [5]. The results are summarized as follows. When films are deposited at a temperature of 200 °C and rate of 0.10 nm/s, those of a very thin thickness of about 1.0 nm are interspersed with amorphous grains, and the amorphous islands gradually expand as the films thicken. Once the film thickness reaches about 5.0 nm, the amorphous region becomes almost continuous and the film is crystallized from the existing crystallites. This type of crystallization at an increased film thickness has been reported for Sb [6–9]. In this paper we begin to collect information on this issue by investigating how the deposition rate influences the crystallization thickness of In_2O_3 films.

The films were reactively deposited using facility and procedure described in ref. [5]. The film deposition rates were 0.02 and 0.22 nm/s, and the oxygen pressure during deposition was about 0.27 Pa. The substrate temperature was kept at about 200 °C. A SiO-coated Cu grid was used as the substrate for the study of the film structure. Films of eight different thicknesses within a range from 1.0 to 7.0 nm were deposited in a single experimental run. The thickness dependence of the film structure was investigated by transmission electron microscopy using JEM 100CX. For the in situ measurements of the electrical resistivity of the films, SiO-coated NaCl crystals were used as substrates. The NaCl crystals were freshly cleaved and optically polished prior to the SiO deposition. The film resistance was determined by the voltage drop between two gold electrodes (about 7 mm wide and 8 mm apart) that had been pre-deposited onto the substrate. The electrical current flowing through the films was below 100 nA.

Figure 1 shows the electron micrographs and electron diffraction patterns of the typical films of four different thicknesses (1.0–4.3 nm) deposited at the rate of 0.02 nm/s. Halo diffraction patterns indicated that the very thin films of about 1.0 nm in thickness were amorphous (Fig. 1a). Specifically, islands of amorphous grains of about 4.0 nm in size were dispersed discontinuously on the substrate. As the film thickened to about 3.0 nm, the amorphous grains gradually grew to a mean size of about 6.0 nm and nearly coalesced. A few of the grains in the 2.0-nm-thick films were crystallized (Fig. 1b: see the arrow in the photograph), and the crystallites grew slightly larger as the films thickened to 3.0 nm.

The diffraction patterns of the 3.8-nm-thick films included both sharp lines and diffuse lines, reflecting an increase in the crystallized regions relative to the amorphous regions (Fig. 1c). Overall, however, the amorphous regions still made up most of the films. The crystallized grains grew to about 20 nm in size, and the number of grains was slightly increased. The dark field images demonstrate that the crystallized grains grew at the expense of

S. Muranaka · N. Hayashi (✉)
Graduate School of Human and Environmental Studies,
Kyoto University, Yoshida-nihonmatsu-cho, Sakyo-ku,
Kyoto 606-8501, Japan
e-mail: hayashi@sou.mbox.media.kyoto-u.ac.jp

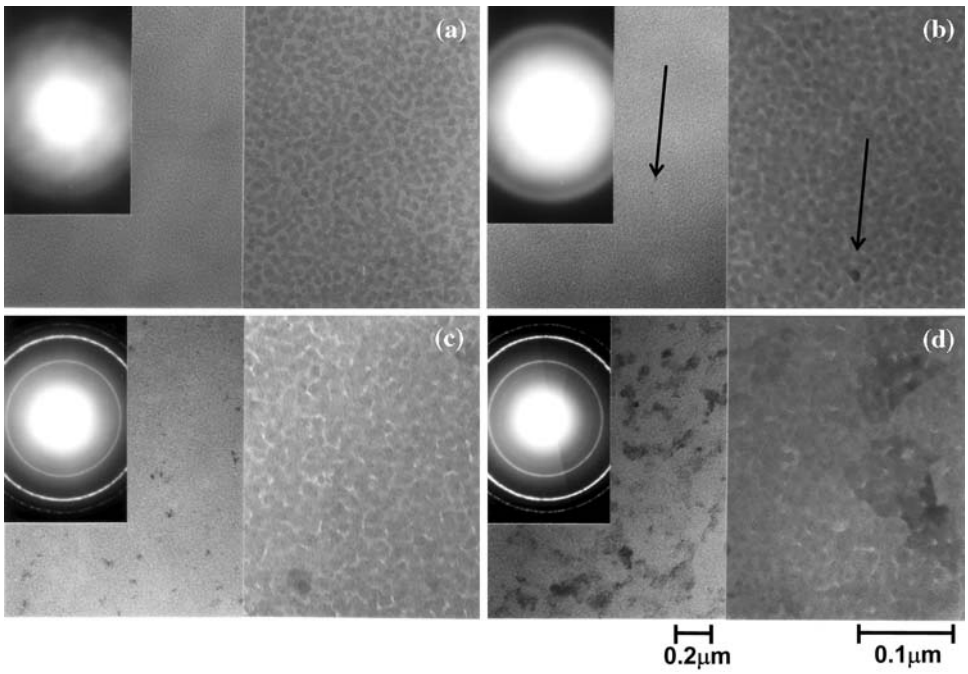

Fig. 1 Electron micrographs and electron diffraction patterns for In_2O_3 films of four different film thicknesses deposited at 0.02 nm/s: **a** 1.0 nm, **b** 2.0 nm, **c** 3.8 nm, **d** 4.3 nm

the surrounding amorphous grains. This crystallization process is very similar to that of films deposited at a rate of 0.10 nm/s [5]. The films were packed densely with the amorphous and crystallized grains, acquiring an almost continuous structure.

Finally, the 4.3-nm-thick films were perfectly crystallized, as indicated by the sharp diffraction lines (Fig. 1d). These films were composed of large crystallized grains grown to a mean size of about 70 nm. Thus, much of the film crystallization took place between the film thicknesses of 3.8 and 4.3 nm, i.e., when the grains coalesced completely, forming an almost continuous structure. Below the film thickness of 3.8 nm, the films only partially crystallized as they thickened.

Figure 2 shows electron micrographs and electron diffraction patterns of typical films deposited at 0.22 nm/s up to films of three different thicknesses, from 2.0 to 7.0 nm. The 2.0-nm-thick films were a mixture of amorphous and crystallized phases, as indicated by the diffuse lines and sharp lines in diffraction patterns (Fig. 2a). The films consisted of islands of amorphous grains of about 7.0 nm, and larger crystallized grains with a mean size of about 12.0 nm. These films were more extensively crystallized than the corresponding films deposited at the lower

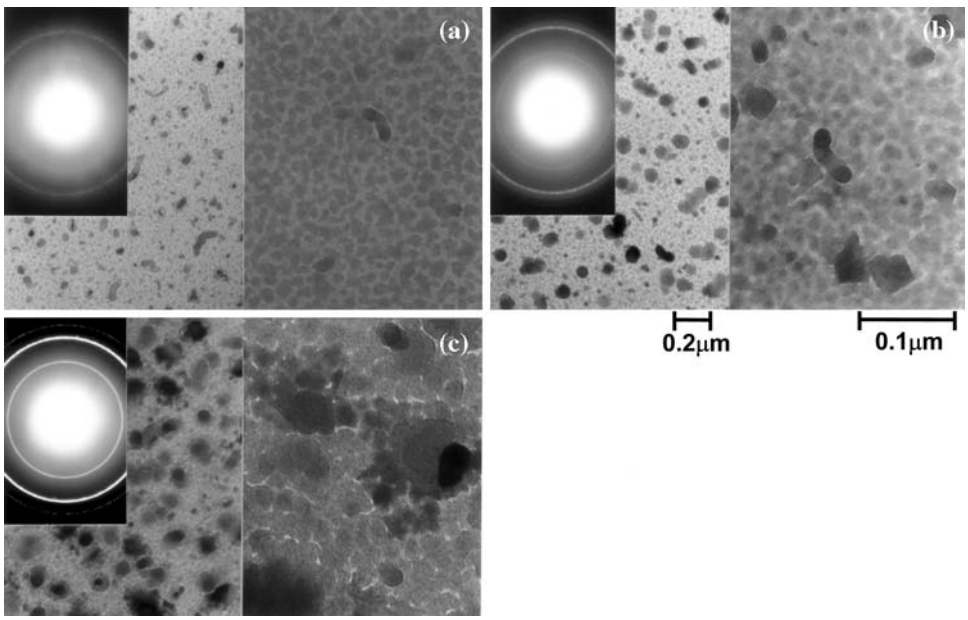

Fig. 2 Electron micrographs and electron diffraction patterns for In_2O_3 films of three different film thicknesses deposited at 0.22 nm/s: **a** 2.0 nm, **b** 6.0 nm, **c** 7.0 nm

deposition rate. That is, the crystallized grains were larger and more numerous, while the amorphous grains were less numerous (see Fig. 1b). At the higher deposition rate, the surface migration of energetic particles increases the statistical probability of crystalline nucleation, resulting in partially crystallized films at the initial stage.

As the film thickened up to about 6.0 nm, the sharp lines in the diffraction patterns became stronger while the diffuse lines weakened, indicating an increase in the crystallized regions relative to the amorphous regions (Fig. 2b). The amorphous grains grew slightly larger, to a mean size about 9.0 nm, in the films of approximately 3.5 nm in thickness, and at higher thicknesses they were almost saturated in size and nearly coalesced. The crystallized grains grew much larger. In the films with thicknesses of 3.5 nm and 6.0 nm; some of the grains grew to about 20 and 40 nm, respectively. Dark field images of the films indicated that the growth of the crystallized grains was similarly induced by the crystallization of neighboring amorphous grains. Finally, the 7.0-nm-thick films were crystallized perfectly, as indicated by the sharp diffraction lines (Fig. 2c). These films consisted of large crystallized grains grown to a mean size of about 120 nm. Thus, the amorphous regions in the films deposited at 0.22 nm/s crystallized at film thicknesses from about 6.0 to 7.0 nm, after the films became almost continuous.

Figure 3 shows the variation of the electrical resistivity at different film thicknesses for films deposited at rates of 0.02 and 0.22 nm/s. The resistance for films deposited at 0.10 nm/s is also presented. The films thinner than 2.0 nm had very high resistivity, above 2 Ωcm, because of their discontinuous structures. As the films thickened, the resistivity of the films deposited at 0.02 nm/s rapidly decreased within the thickness range from about 2.0 to 4.5 nm. In contrast, the resistivities of the films deposited at rates of 0.10 and 0.22 nm/s decreased at the thicker stage from about 3.0 to 5.0 nm and 3.5 to 7.0 nm, respectively. Beyond the critical film thicknesses of 4.5, 5.0, and 7.0 nm for the films deposited at rates of 0.02, 0.10, and 0.22 nm, respectively, the resistivity of each film remained almost steadily unchanged. The initial decrease in the film resistivity was induced by the formation of the network of grains for the electro-conductive paths in the films, as indicated by electron microscopy observation (see Fig. 1b, Fig. 2c in ref. [7], and Fig. 2b). The film thicknesses for the initial decrease in resistivity agreed well with those of the films reported by other authors (1.5–4.0 nm) [10, 11]. The steady resistivity beyond the critical film thicknesses indicated that the films were entirely continuous. These film thicknesses in the resistivity curves corresponded closely with the crystallization thicknesses of the films determined from observations by transmission electron microscopy. Thus, the films were completely crystallized as they became entirely continuous.

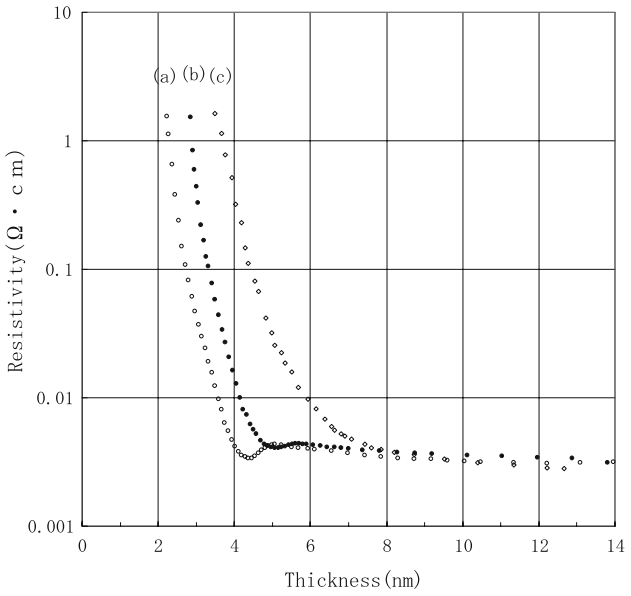

Fig. 3 Variation of electrical resistivity with film thickness for three kinds of films. The films were deposited at rates of (a) 0.02 nm/s, (b) 0.10 nm/s, and (c) 0.22 nm/s

The results of our experiments indicate that the films were initially amorphous or quasi-amorphous, with islands of grains, and collectively crystallized at the film-growth stage as they became almost continuous. The disordered structure of a film at the initial stage results from the quenching of the particles deposited on the substrate or from the drastically reduced surface migration of adatoms [12]. In the subsequent stage of the film growth, the amorphous state is maintained by the interaction with the substrate based on the van der Waals forces. The film surface of the vacuum side or the grain surface also tends to prevent the films from crystallizing [6, 7]. This surface effect is weakened as the film thickens, because the volume fraction near the film surface is lower than that inside the film. At the critical film thickness in our experiments, the grains coalesced into an almost continuous film. In the films composed of connected grains with adequate thickness, the heat released from the local crystallization of the amorphous grains is presumably transferred effectively to the neighboring grains, inducing them to crystallize. This process advances grain by grain, propagating through the film and culminating in a collective crystallization. This mechanism of crystallization via heat transfer has also been proposed by Kaiser in a study on Sb films [8].

The crystallization of the films occurred at the thicker stage as the deposition rate increased. This was probably the result of the active surface-migration of the particles deposited at the higher deposition rate. The active migration of adatoms increases the likelihood that particles will stick to stable sites, that is, to crystallized grains, while the

growth of the amorphous grains remains relatively retarded. The slow growth of the amorphous grains results in the formation of the grains network at the higher film thicknesses, and correspondingly to the crystallization at the thicker stages.

References

1. Muranaka S, Bando Y, Takada T (1987) Thin Solid Films 151:355
2. Wulf H, Quaas M, Steffen H, Hippler H (2000) Thin Solid Films 377:418
3. Rogozin A, Shevchenko N, Vinnichenko M, Prokert F, Cantelli V, Kolitsch A, Moller W (2004) Appl Phys Lett 85:212
4. Adurodija FO, Semple L, Bruning R (2006) J Mater Sci 41:7096. doi:10.1007/s10853-006-0038-3
5. Muranaka S (1991) Jpn J Appl Phys 30:L2062
6. Kinbara A, Ohmura M, Kikuchi A (1967) Thin Solid Films 34:37
7. Hashimoto M (1984) Thin Solid Films 116:373
8. Kaiser N (1984) Thin Solid Films 116:259
9. Hoareau A, Hu JX, Jensen P, Melinon P, Treilleux M, Cabaud B (1992) Thin Solid Films 209:161
10. Korobov V, Leibovitch M, Shapira Y (1994) Appl Phys Lett 65:2290
11. Sun XW, Huang HC, Kwok HS (1996) Appl Phys Lett 68:2663
12. Chopra KL (1969) Thin film phenomena. McGraw-Hill, New York, p 195